AIP | Applied Physics Letters

Origin of photomultiplication in C 60 based devices

Jinsong Huang and Yang Yang

Citation: Applied Physics Letters **91**, 203505 (2007); doi: 10.1063/1.2807278
View online: http://dx.doi.org/10.1063/1.2807278
View Table of Contents: http://scitation.aip.org/content/aip/journal/apl/91/20?ver=pdfcov
Published by the AIP Publishing

Origin of photomultiplication in C_{60} based devices

Jinsong Huang[a] and Yang Yang[b]
Department of Materials Science and Engineering, University of California-Los Angeles, 405 Hilgard Av., Los Angeles, California 90095, USA

(Received 8 October 2007; accepted 19 October 2007; published online 13 November 2007)

In this manuscript, the origin of the photomultiplication effect was studied in C_{60} based devices by evaluating the wavelength dependent external and internal quantum efficiencies under various biases. The effect of materials with disordered structures on the photomultiplication effect was determined by intentionally integrating both ordered and disordered material structures into one organic solar cell device with a configuration of indium tin oxide/poly(3,4-ethylenedioxythiophene) poly(styrenesulfonate) (PEDOT:PSS)/pentacene/C_{60} fullerene/bathocuproine (BCP)/Al. Our results show that both the disordered structure of C_{60} and the charge trapping effect at the C_{60}/PEDOT:PSS interface contribute to the photomultiplication effect. By studying the C_{60}-only single layer device, the charge trapping sites are identified to be at the C_{60} and PEDOT:PSS interface. The interfacial traps behave as an electronic valve that enables a significant increase in electron injection, which causes the photomultiplication phenomena. Quantitative comparisons indicate that photomultiplication induced by C_{60} disordered structure is much less significant than that by charge trapping at the interface. © *2007 American Institute of Physics*.
[DOI: 10.1063/1.2807278]

The phenomenon of the photomultiplication (PM) effect has been intensively applied in highly sensitive photonic detectors. The gain of detectors, defined by the ratio of the number of carriers extracted from the device to the circuit and the number of incident photons, is much higher than 100% in PM devices, such as avalanche photodiodes (APDs). The PM effect in inorganic semiconductor APDs is generally induced by impact ionization of the semiconductor under high reverse bias (typically 100–200 V in silicon based APDs). The PM phenomenon in organic semiconductor devices was recently observed by several groups.[1–5] These devices have either a single organic layer[1,2] or double organic layers[1,5] sandwiched by metal electrodes. It is interesting from a scientific and applied point of view to understand the origin of this PM in organic diodes. Unlike in inorganic semiconductors, impact ionization should not be the mechanism for PM in such organic devices. In contrast to the low localization energy of inorganic semiconductors such as silicon, which is typically in the range of meV, organic materials generally have a rather high exciton binding energy [typically 0.1–1.4 eV (Ref. 6)], which requires electrical fields that are two to three orders of magnitude higher to convert electrons from localized states into ionized states. However, PM was observed in organic devices under only a few volts of bias, as shown in the results detailed in the later part of this paper. The applied electrical field is much smaller than that required for achieving ionization, and hence, there must be some other mechanism(s) responsible for the PM in organic diodes. Several models have been proposed, such as increased charge injection due to the field-activated structural traps at the interface[2–5] and photocurrent multiplication by exciton energy transfer to trapped carriers in the bulk material.[1] The actual mechanism is still not clear, and to a certain degree, it is still under debate. One limitation in PM measurements is the inability to determine the PM factor at a function of wavelength. Therefore, the origin of the photocurrent could not be associated with or referred to as a specific material's property in the multilayer device structure.

In this manuscript, we aim to understand the mechanism for the PM phenomenon in organic diodes using incident photon to current efficiency (IPCE) measurements.[7] It is shown that, by combining IPCE and optical absorption results of the materials, the contribution from each material to the PM effect can be identified. Therefore, the origin of the PM effect can be identified.

The material adopted in this experiment for PM is C_{60}, which is one of the most commonly used acceptor materials in organic solar cells. C_{60} was chosen due to its high degree of rotational disorder.[8,9] The PM phenomenon was observed in a typical solar cell device with the structure of ITO (150 nm)/PEDOT:PSS (25 nm)/pentacene (10–50 nm)/C_{60} (30 nm)/BCP (8 nm)/Al (100 nm), where ITO is indium tin oxide, PEDOT:PSS is poly(3,4-ethylenedioxythiophene) poly(styrenesulfonate), and BCP is bathocuproine. Solar cells using this structure have been demonstrated to be highly efficient due to the long exciton diffusion length in pentacene.[10] The other reason that pentacene is adopted is that, in contrast with C_{60}, it can form very good crystalline or ordered structures.[11] This device contains materials with a disordered structure (C_{60}) and an ordered structure (pentacene); hence, it is ideal to realize the influence of material structure on the PM effect. In our experiment, internal quantum efficiency was chosen to distinguish contributions of short circuit current from C_{60} and pentacene. The internal quantum efficiency $\eta_{IQE}(\lambda)$ (Ref. 12) was obtained based on the following equation:

$$\eta_{IQE}(\lambda) = \eta_{EQE}(\lambda)/\mathrm{abs}(\lambda), \quad (1)$$

where $\eta_{EQE}(\lambda)$ is external quantum efficiency, or IPCE, and abs(λ) is the absorbance of active layer. It is generally, the

[a]Present address: Agiltron, Inc., Boston, MA. Electronic mail: jhuang@agiltron.com
[b]Electronic mail: yangy@ucla.edu

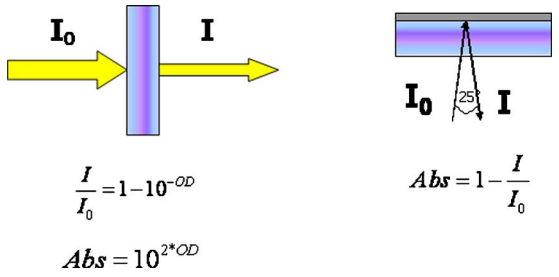

FIG. 1. (Color online) Diagram for the absorption measurement by transmission method and reflection method.

transmitted absorption is used to characterize the absorption of thin films. As shown in Fig. 1, in the transmitted absorption measurement, the absorbance is calculated by considering the optical loss due to the absorption of the organic films; the equation is given in Fig. 1. It is found in our experiment that the wavelength dependent absorption curve shape obtained from direct transmitted-type absorption measurement is much different from our EQE curve. Such deviations are believed to be due to the optical interference effect in the thin films of our device. Therefore, in order to obtain a more accurate absorption data, we adopted a reflective-type absorption method.[13] In this measurement, as illustrated in Fig. 1, a large area device was measured with a piece of Al coated ITO glass as reference. The absorbed light is the difference between the incident light and the reflected light. Therefore, through this method, the optical interference is considered and the absorption measurement is closer to real values. The absorption from pure C_{60} or pentacene is shown in Fig. 2(a). As one can see from the absorption spectrum of C_{60} and pentacene, the maximum absorption of pentacene is located at 670 nm, where there is barely any absorption by C_{60}. Hence, nearly all contributions for internal (or external) quantum efficiency at 670 nm come from pentacene. On the

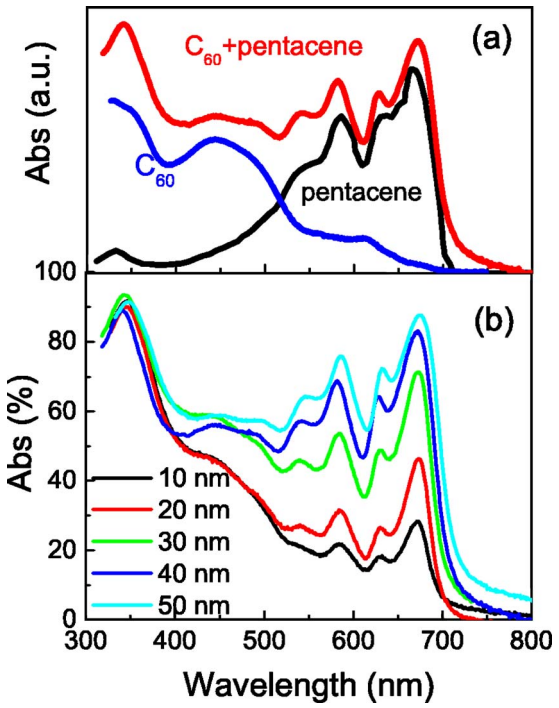

FIG. 2. (Color online) (a) Absorption of pure C_{60} and pentacene and (b) absorption of solar cell devices with petacene thickness in the range of 10–50 nm.

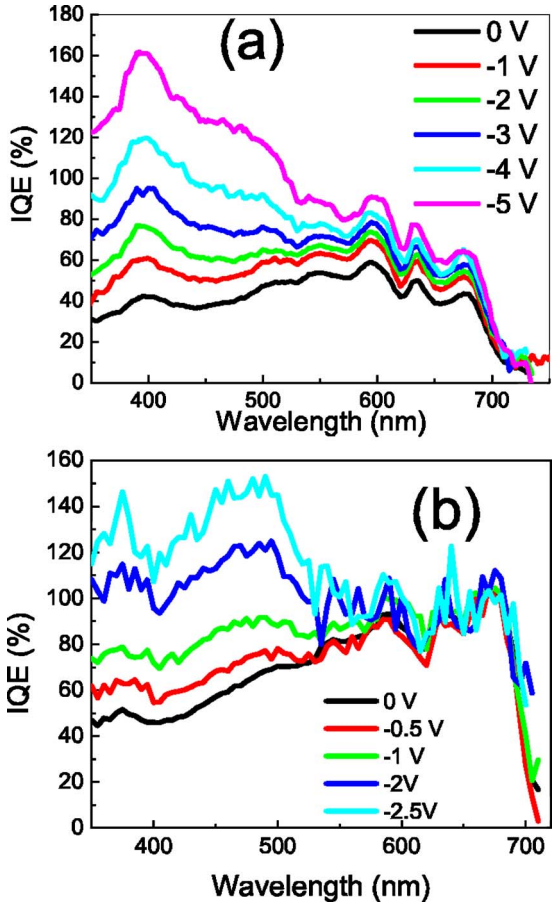

FIG. 3. (Color online) Internal quantum efficiency of solar cell devices with pentacene thicknesses of (a) 40 nm and (b) 10 nm under various biases.

other hand, in the wavelength range between 300 and 550 nm, most absorption comes from C_{60}. Therefore, by comparing the internal quantum efficiency at these two different wavelength regions, the effect of disordering on PM can be easily separated. Figure 2(b) shows the measured absorption curves for devices with pentacene thickness in the range of 10–50 nm with other same parameters.

During the IPCE measurement, the devices were reverse biased so that all excitons generated by the incident photons can be collected. Figure 3(a) shows the $\eta_{IQE}(\lambda)$ calculated from Eq. (1) under different biases for solar cell devices with pentacene thickness of 40 nm. It can be seen clearly that IQE at 300–550 nm (C_{60} absorption) increases with increasing applied reverse voltage, and it exceeds 100% when the bias is larger than 4 V. The $\eta_{IQE}(\lambda)$ at 670 nm (pentacene absorption) also increases with increasing reverse bias voltage. The difference of $\eta_{IQE}(\lambda)$ between C_{60} and pentacene is that pentacene tends to saturate at higher voltages. This can be explained by the incomplete exciton dissociation in pentacene resulting from the fact that the exciton diffusion length is less than the pentacene film thickness (40 nm in this device). In order to prove this, the thickness of pentacene was reduced to 10 nm, while other parameters were left unchanged for a controlled device. It is expected that all excitons in such thin pentacene film should dissociate because the exciton diffusion length in pentacene is much larger than 10 nm.[10] As one can see from Fig. 3(b), internal quantum efficiency reaches 100% at 670 nm even under zero bias condition. Once more, the EQE does not increase with the applied reverse bias,

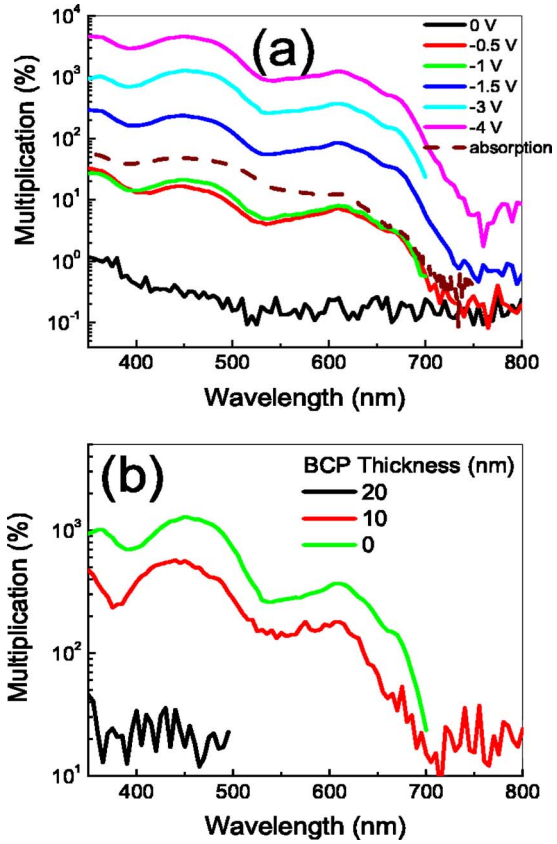

FIG. 4. (Color online) External quantum efficiency of devices (a) PEDOT (25 nm)/C_{60} (80 nm)/BCP (8 nm)/Al and (b) PEDOT/BCP (0–20 nm)/C_{60} (80 nm)/BCP (8 nm)/Al under various biases.

which means all excitons have dissociated and been collected by the electrodes. This agrees with our expectation very well. However, the dependence of IQE with applied voltage is much different in the wavelength range of 300–550 nm, where the absorption mainly comes from C_{60}. IQE continues to increase with applied negative driving voltage and exceeds unit under −2.5 V bias. Therefore, it is obvious that the PM phenomenon is from C_{60} rather than from pentacene in the same device, which should be attributed to the different degrees of disorder in these two materials. This experiment verifies that energetic disorder could be the origin of the PM phenomenon. However, we noticed that the PM factor in this device is much less than what Reynaert *et al.*[1] and Hiramoto *et al.*[3] observed with slightly different device structures. Since the formula proposed by Reynaert *et al.* predicts a small PM factor at a high bias of 10 V, it is questionable if the disorder is the origin of high PM factors in other experiments.

In order to further study the dominating mechanism for the PM effect, the pentacene layer in the device was removed from our device structure, and the C_{60}-only single active layer devices were studied. The devices fabricated have the structure of ITO (150 nm)/PEDOT:PSS (25 nm)/C_{60} (80 nm)/BCP (8 nm)/Al (100 nm). Figure 4(a) shows the IPCE results measured under reverse bias from 0 to −4 V. The EQE at zero bias is much smaller than that in the solar cell device because there is no exciton dissociation driving force (the donor-acceptor system) in this device. The applied electrical field helps the exciton dissociation and increases the EQE to 30% at −0.5 V bias. The EQE quickly exceeds unit at −1.2 V bias and increases dramatically with the applied reversed bias. The maximum EQE exceeds 5000% at −4 V bias. The EQE can be correlated to absorption very well, meaning that all generated charges or PM phenomena are related to C_{60} rather than BCP. This high PM factor must relate to the new interface (PEDOT:PSS/C_{60} interface) introduced after removing the pentacene layer rather than from the C_{60} bulk. In order to verify this, a second BCP layer is inserted between C_{60} and PEDOT:PSS. As one can see from Fig. 4(b), the PM factor is reduced significantly after a 10 nm BCP intermediate layer is inserted and is completely suppressed after a 20 nm BCP insertion. It is direct evidence that the PM phenomenon in this type of C_{60} device comes from the PEDOT:PSS interface rather than the C_{60} bulk.

The detailed PM mechanism can be described as the following. Upon photoexcitation, photogenerated exciton forms in the C_{60} bulk layer. Excitons dissociate driven by applied electrical field. Electrons will drift to the Al electrode, but holes are trapped at the PEDOT:PSS and C_{60} interface. This high density of trapped holes will reduce the electron injection barrier from PEDOT:PSS and will eventually lead to strong electron injection from PEDOT:PSS to C_{60}. As a result, the PEDOT:PSS and C_{60} interface acts as a dynamic electronic valve for electron injection. Incident photons can switch on this valve. PM occurs when, on average, more than one electron are injected from PEDOT:PSS to C_{60} per incident photon. The PM factor can be very high at low biases because the charge injection is an exponential function of the charge injection barrier, which has a linear relationship with number of incident photons (or trapped charges).

In summary, we have observed the PM phenomenon, which results from both disorder in bulk materials (C_{60}) and interfacial charge trapping (PEDOT:PSS/C_{60}). This result provides important guidelines for future development of low-operation-voltage organic photodetectors.

The financial support of this work is from the Air Force Office of Scientific Research (FA9550-07-1-0264). The technical discussions with Prof. Michael McGehee of Stanford University are also deeply appreciated.

[1] J. Reynaert, V. I. Arkhipov, P. Heremans, and J. Poortmans, Adv. Funct. Mater. **16**, 784 (2006).
[2] M. Hiramoto, T. Imahigashi, and M. Yokoyama, Appl. Phys. Lett. **64**, 187 (1994).
[3] M. Hiramoto, A. Miki, M. Yoshida, and M. Yokoyama, Appl. Phys. Lett. **81**, 1500 (2002).
[4] T. Katsume, M. Hiramoto, and M. Yokoyama, Appl. Phys. Lett. **69**, 3722 (1996); G. Matsunobu, Y. Oishi, M. Yokoyama, and M. Hiramoto, *ibid.* **81**, 1321 (2002).
[5] K. Nakayama, M. Hiramoto, and M. Yokoyama, Appl. Phys. Lett. **76**, 1194 (2000).
[6] S. F. Alvarado, P. F. Seidler, D. G. Lidzey, and D. D. C. Bradley, Phys. Rev. Lett. **81**, 1082 (1998).
[7] G. Li, V. Shrotriya, J. Huang, Y. Yao, T. Moriarty, K. Emery, and Y. Yang, Nat. Mater. **4**, 864 (2005).
[8] P. A. Heiney, J. E. Fischer, A. R. McGhie, W. Romanow, A. Denenstein, J. McCauley, Jr., and A. Smith, Phys. Rev. Lett. **66**, 2911 (1991).
[9] R. C. Yu, N. Tea, M. B. Salamon, D. Lorents, and R. Malhotra, Phys. Rev. Lett. **68**, 2050 (1992); X. Sun, G. P. Zhang, Y. S. Ma, R. L. Fu, and X. C. Shen, Phys. Rev. B **53**, 15481 (1996).
[10] S. Yoo, B. Domercq, and B. Kippelen, Appl. Phys. Lett. **85**, 5427 (2004).
[11] S. Lee, B. Koo, J. Shin, E. Lee, H. Park, and H. Kim, Appl. Phys. Lett. **88**, 162109 (2006).
[12] S. A. McDonald, G. Konstantatos, S. Zhang, P. W. Cyr, E. J. D. Klem, L. Levina, and E. H. Sargent, Nat. Mater. **4**, 138 (2005).
[13] J. Y. Kim, S. H. Kim, H. H. Lee, K. Lee, W. Ma, X. Gong, and A. J. Heeger, Adv. Mater. (Weinheim, Ger.) **18**, 572 (2006).